Chapter 10
Characterization of Fracture Behavior of Multi-Walled Carbon Nanotube Reinforced Cement Paste Using Digital Image Correlation

Nima Zohhadi, Behrad Koohbor, Fabio Matta, and Addis Kidane

Abstract This paper reports on the fracture behavior of MWCNT-reinforced cement paste based on evidence from three-point bending tests of single-edge notched beam samples. Digital image correlation (DIC) was used to measure full-field displacements at different stages of fracture in reinforced and unreinforced samples. Strain maps extracted from displacement data were used to characterize the morphology of the fracture process zone (FPZ). The DIC principal tensile strain maps from nanoreinforced samples consistently highlighted the development of a larger FPZ prior to failure. Evidence from scanning electron microscopy analysis of fracture surfaces further supports the hypothesis that highly-dispersed and well-bonded MWCNTs contribute to toughness through crack-bridging.

Keywords Cement paste • Digital image correlation • Fracture properties • Carbon nanotubes

10.1 Introduction

The physical and mechanical properties of carbon nanofilaments and nanotubes, such as multi-walled carbon nanotubes (MWCNTs), make them suitable as a chemically compatible internal reinforcement for the strengthening and toughening of otherwise quasi-brittle cement-based composites [1]. The main challenges in the incorporation of MWCNTs in cement composites are to attain a uniform dispersion within the composite matrix as well as an effective chemical bond with cement hydrates [2]. Due to their high hydrophobicity and attractive Van der Waals forces MWCNTs tend to agglomerate and form entangled aggregates [3]. As a result a stable and homogeneous dispersion of nanotubes cannot be obtained without functionalization [4]. In addition, due to the small dimensions of MWCNTs, mechanical bonding and physical anchorage can hardly be relied upon, and the primary bonding mechanism is reasonably due to the formation of chemical bonds between the functionalized MWCNTs and the cement matrix [5].

Several functionalization techniques have been proposed by different researchers to address these challenges. The most common methods include: ultrasonication [6], acid-functionalization [7], and surfactant-coating [8]. Among these techniques acid-functionalization is preferred since the formation of chemically active carboxyl (COOH) and hydroxyl (OH) groups attached to the surface of MWCNTs facilitate the formation of covalent bonds with the cement hydrates [9]. Once uniform dispersion and effective bonding are achieved, MWCNTs can act as reinforcement for cementitious composites [10]. Previous research focused mainly on the effect of MWCNTs on compressive and flexural strength of cement paste and mortar, as well as physicochemical properties such as early-age shrinkage [11], porosity [12], and electrical conductivity [13]. For example, Li et al. [14] reported up to 19 and 25 % enhancement in compressive and flexural strength of mortar with the addition of 0.5 % in weight of cement (herein denoted as '%') acid-treated MWCNTs. Manzur et al. [15] used ultrasonication to disperse

N. Zohhadi (✉) • F. Matta
Department Civil and Environmental Engineering, University of South Carolina, 300 Main St., Columbia, SC, USA
e-mail: zohhadi@email.sc.edu; fmatta@sc.edu

B. Koohbor • A. Kidane
Department of Mechanical Engineering, University of South Carolina, 300 Main St., Columbia, SC, USA
e-mail: koohbor@email.sc.edu; kidanea@cec.sc.edu

J. Carroll and S. Daly (eds.), *Fracture, Fatigue, Failure, and Damage Evolution, Volume 5: Proceedings of the 2014 Annual Conference on Experimental and Applied Mechanics*, Conference Proceedings of the Society for Experimental Mechanics Series,
DOI 10.1007/978-3-319-06977-7_10,

0.3 % MWCNTs in mortar and obtained up to 29 % increase in compressive strength. In another study, incorporation of 0.048 % surfactant-treated MWCNTs increased the fracture load and Young's modulus of cement paste by 25 % and 40 %, respectively [16].

This paper presents early experimental evidence from an ongoing project aimed at investigating the effect of highly-dispersed acid-functionalized MWCNTs on the fracture behavior of cement paste. First, the homogeneous distribution of MWCNTs in cement mortar was verified based on evidence from compressive strength characterization and scanning electron microscopy (SEM) analysis of plain and nanoreinforced mortar samples. The effect of MWCNTs on fracture characteristics of cement paste was studied by means of three-point bending tests of single-edge notched beams. Digital image correlation (DIC) was enlisted to obtain full-field displacement maps in the notch region. Strain maps extracted from the displacement data were used to study the effect of MWCNTs on the morphology of the fracture process zone (FPZ).

10.2 Experimental Program

10.2.1 Materials

Ordinary Portland cement (OPC) Type I and ASTM C778 silica sand were used to fabricate the specimens. The MWCNTs (Cheap Tubes Inc, cat# sku-030101, Brattleboro, VT) were used as-received. Salient properties of the MWCNTs as provided by the supplier are presented in Table 10.1.

10.2.2 Preparation of MWCNT-Reinforced Cement Paste and Mortar

The MWCNTs were dispersed in water and the resulting suspension was mixed with cement (and sand in case of the mortar cubes used for the characterization of compressive strength) in accordance with ASTM C305. To enhance dispersion in water and bonding with cement hydrates, MWCNTs were first functionalized using an acid-treatment technique.

In a typical procedure, the MWCNTs were soaked in an aqueous solution containing ammonium persulfate, $(NH_4)_2S_2O_8$ (Sigma Aldrich, cat# 215589) and sulfuric acid, H_2SO_4 (Sigma Aldrich, cat# 339741) and the resulting suspension was stirred for 24 h using a magnetic stirrer. The resulting solution was sonicated for 10 min using an ultrasonic processor (S-4000 Ultrasonic Processor, Misonix, Inc., Farmingdale, NY) to mechanically separate nanotube clusters and ensure that the acids reach the innermost nanotubes. The solution was then stirred for another 24 h. At this point, the MWCNTs reached a pH of about 1 and were not suitable for mixing with cement. Therefore, the MWCNTs were washed with deionized water to raise the pH to 7, and then dried and stored as dry powder. The acid-functionalized MWCNTs were added to water and sonicated for 20 min before incorporating them in the cement mixtures for mortar (used to fabricate the compression test samples) and cement paste (used to fabricate the fracture mechanics test samples).

10.2.3 Specimens, Test Setup and Protocol

Compressive strength characterization—The effect of functionalized MWCNTs on the compressive strength of cement mortar was evaluated using compression tests on 2-in. (50-mm) cube specimens in agreement with ASTM C109. The specimens were fabricated with mortar having OPC:sand:water weight proportion of 1:2.75:0.484 in agreement with ASTM C109. Two reinforcement concentrations of 0.05 and 0.5 % were used to prepare three specimens per group. The specimens were moist-cured for 24 h and then demolded and kept under saturated lime water until the age of 28 days. Compression tests were performed using a test frame (MTS 810 Material Testing System, MTS Systems Inc., Eden Prairie, MN) under displacement-control mode with a displacement rate of 0.625 mm/min.

Visual characterization of MWCNT dispersion in mortar—The dispersion of acid-treated MWCNTs in cement mortar was investigated by means of SEM analysis of samples collected from fracture surfaces of failed cube specimens. SEM

Table 10.1 Properties of as-received MWCNTs

Outer diameter [nm]	Inner diameter [nm]	Specific surface area [m^2/g]	Length [μm]	Purity [%]
<8	2–5	500	10–30	>95

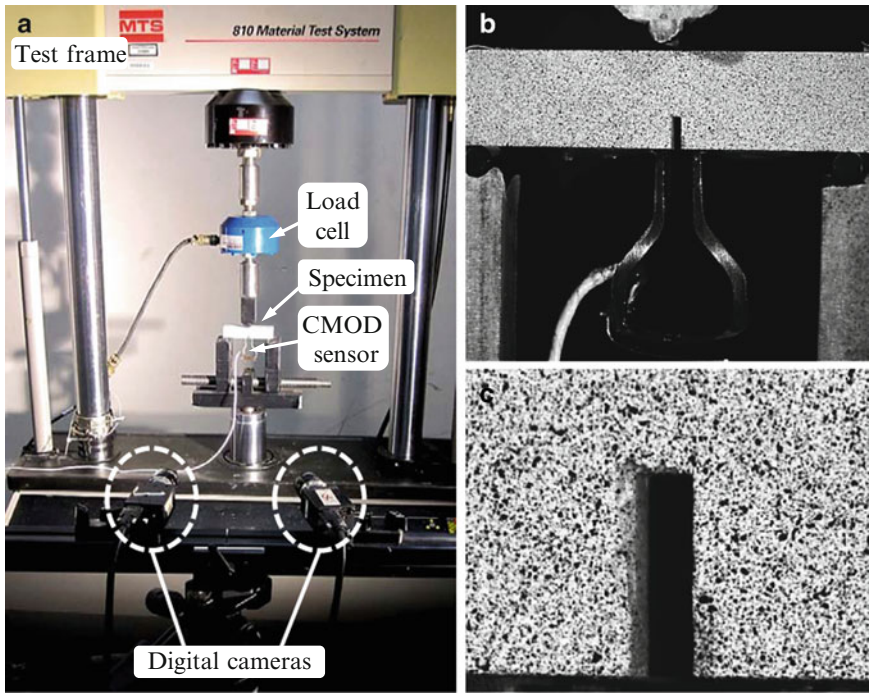

Fig. 10.1 Fracture mechanics testing and DIC measurement: (**a**) test setup; (**b**) close-up photograph of notched beam specimen; and (**c**) close-up view of speckle pattern around 2 × 6 mm notch

micrographs were acquired using a Zeiss Ultra Plus Field Emission Scanning Electron Microscope. All samples were oven-dried for 24 h at 60 °C and gold-sputtered prior to being tested.

Fracture mechanics characterization—The experimental evidence to assess the effect of MWCNTs on the fracture behavior of cement paste was obtained by means of three-point bending test on single-edge notched beam specimens with dimensions of 20 × 20 × 80 mm, as illustrated in Fig. 10.1. Two reinforcement concentrations of 0.05 and 0.5 % were considered and three specimens per group were fabricated. A 0.5 w/c ratio was used for the Type I OPC paste. Specimens were moist-cured for 24 h and then demolded and kept under saturated lime water until the age of 28 days. A water-cooled diamond saw was used to cut 6-mm long and 2-mm wide notches at midspan (Fig. 10.1b, c). A clip gage was used to measure the crack mouth opening displacement (CMOD). The load tests were performed in displacement-control mode at a rate of 0.01 mm/min.

DIC measurements—A thin layer of white wash was applied on the surface of the specimens and a dark speckle pattern was then spray-painted on the white washed background (Fig. 10.1b, c). A pair of five MP cameras (Grasshopper GRAS-50S5M-C, Point Grey, Richmond, Canada) equipped with 35-mm lenses was utilized to acquire images at a 5 fps rate (Fig. 10.1a). The DIC analysis was performed using the software Vic-3D (v7, Correlated Solutions Inc., Columbia, SC) using a subset size of 49 × 49 pixels with a step of 15 pixels.

10.3 Results and Discussion

10.3.1 Compressive Strength

The increase in compression strength is greatly affected by the dispersion of carbon nanoreinforcement [6, 15], and was used as an indirect means to assess the effectiveness of the functionalization technique. Poorly-dispersed MWCNTs tend to produce defect sites at the locations of entangled MWCNTs, thereby contributing to reducing the compressive strength [15]. A summary of the compression test results is presented in Table 10.2.

All nanoreinforced mortar specimens consistently exhibited a higher compressive strength than the counterpart plain mortar specimens, suggesting that a homogeneous dispersion was attained. The strength gain increased for the higher nanoreinforcement concentration (0.5 % in weight of cement). The average strength increased by 24 % and 41 % for MWCNT additions of 0.05 % and 0.5 %, respectively.

Table 10.2 Results of compression tests

Group	Compressive strength [MPa]	Δ [%]
Control	32 ± 3	–
MWCNT 0.05 %	39 ± 1	24
MWCNT 0.5 %	44 ± 4	41

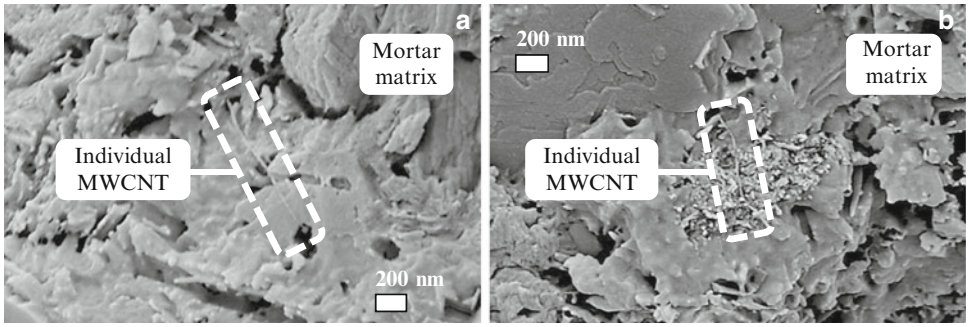

Fig. 10.2 Dispersion of MWCNTs in cement mortar at different concentrations: (**a**) 0.05 %; and (**b**) 0.5 %

Table 10.3 Results of fracture mechanics tests

Specimen group	Maximum load [N]	Stiffness [N/mm]
Control	111 ± 3	4,862 ± 276
MWCNT 0.05 %	139 ± 16	9,400 ± 1,060
MWCNT 0.5 %	135 ± 12	8,981 ± 1,465

10.3.2 SEM Analysis

Portions of fracture surfaces of failed mortar cubes were inspected via SEM to assess the dispersion of MWCNTs in the cement composite. Representative micrographs are presented in Fig. 10.2.

At both 0.05 and 0.5 % concentrations MWCNTs were mostly found as individual nanotubes, indicating that a satisfactory dispersion was attained. In addition, at the majority of the locations inspected, MWCNTs were found partially embedded in cement hydrates, indicating a good chemical compatibility between the acid-functionalized nanoreinforcement and the cement matrix.

10.3.3 Flexural Strength, Stiffness, and Fracture Behavior

The effect of highly-dispersed MWCNTs on the flexural response and fracture characteristics of cement paste was studied by means of three-point bending tests of single-edge notched beams. A summary of the test results is presented in Table 10.3.

The incorporation of MWCNTs in concentrations of 0.05 % and 0.5 % led to an increase in the average maximum load of 25 % and 22 %, respectively, and an increase in the average stiffness of 93 % and 85 %, respectively, consistent with the strength enhancement obtained for mortar cubes. A major stiffness increase was also reported by other researchers [16] and may be attributed primarily to a reduced porosity and refinement of the pore structure [12, 13, 17], which may not further improve at increasing MWCNT concentrations in part due to the difficulty to consistently ensure uniform dispersion.

Representative examples of load-CMOD response of unreinforced and nanoreinforced notched beams are presented in Fig. 10.3. The significant stiffness increase for MWCNT-reinforced samples can be clearly noted. The unreinforced control specimens experienced a sudden drop in the load resisted after attaining the maximum (peak) load, whereas the nanoreinforced specimens exhibited a more progressive damage development and retained a higher residual strength past the peak load.

To better understand the influence of MWCNTs, the load-CMOD curves were divided in three stages: linear elastic, non-linear pre-peak load, and post-peak load. For each group, Table 10.4 compares the energy absorbed in these three stages. A 15 % deviation from linearity in the slope of the load-CMOD curves was used to determine the beginning of the non-linear pre-peak load stage.

The energy absorbed in the stiffer nanoreinforced samples in the linear elastic stage was on average smaller than that in the unreinforced specimens. However, in the second stage (non-linear pre-peak) where nano-cracks form and coalesce into

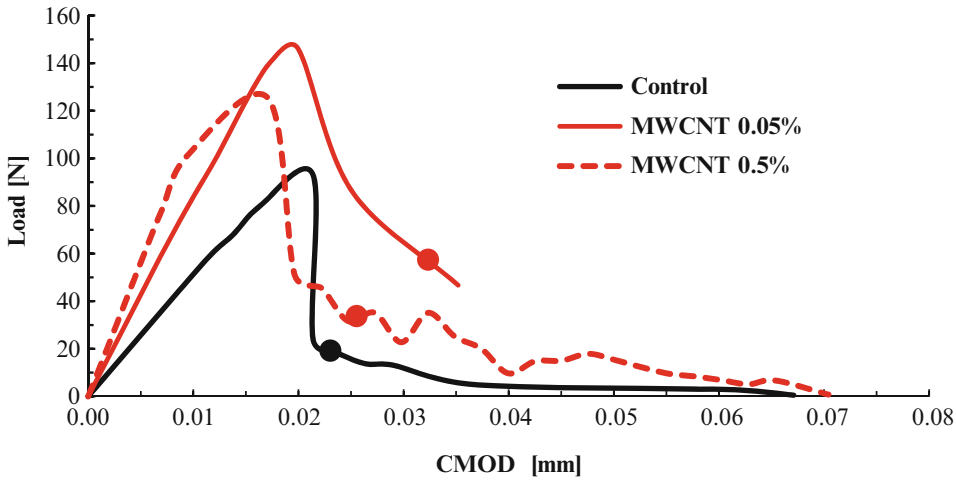

Fig. 10.3 Representative load-CMOD curves. Markers indicate load-CMOD coordinates for DIC strain maps in Fig. 10.5

Table 10.4 Energy at different stages of load-CMOD curve

Specimen group	Total energy [N-mm]	Linear elastic	Non-linear pre-peak load	Post-peak load
Control	1.63 ± 0.05	0.79 ± 0.09	0.38 ± 0.10	0.46 ± 0.08
MWCNT 0.05 %	2.14 ± 0.70	0.60 ± 0.47	0.60 ± 0.24	0.94 ± 0.67
MWCNT 0.5 %	2.09 ± 0.54	0.59 ± 0.10	0.56 ± 0.24	1.08 ± 0.46

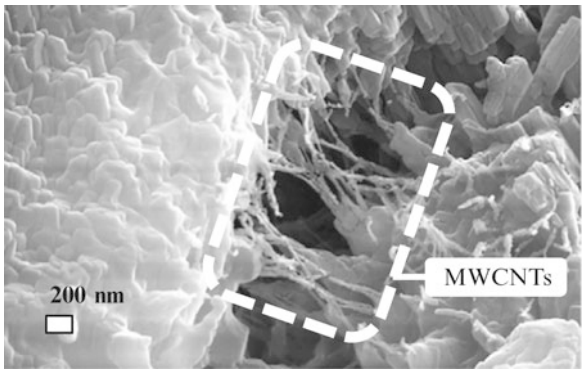

Fig. 10.4 SEM micrograph showing potential crack-bridging contribution of MWCNTs in cement paste

micro-cracks, the energy was significantly higher for the reinforced samples. This behavior is reasonably attributed to the presence of well-dispersed MWCNTs, which may contribute to enhancing the fracture toughness through a crack- or defect-bridging effect, similar to that provided at a larger scale by micro-fiber reinforcement in fiber-reinforced cement composites, as suggested the SEM micrograph in Fig. 10.4.

Defect- and crack-bridging action requires effective bonding between the nanoreinforcement and the surrounding cement paste, and the rupture and progressive pull-out of well-bonded MWCNTs can contribute to fracture toughness [13]. In fact, the influence of MWCNTs is more evident in the third stage of the load-CMOD curve (post-peak load), thus past the maximum load, where unreinforced specimens rapidly collapse. The average energy absorbed in the post-peak load stage by specimens reinforced with 0.05 % and 0.5 % MWCNTs was 104 % and 135 % higher than the unreinforced specimens, respectively, highlighting the toughening contribution of well-dispersed and bonded MWCNTs. As a result, the total energy increased by 31 % and 28 % in the case of nanoreinforced specimens with 0.05 % and 0.5 % MWCNTs, respectively.

10.3.4 Fracture Process Zone

The fracture process zone (FPZ) is the intermediate space between the cracked and uncracked regions ahead and around the crack tip [18]. The effect of MWCNTs on the FPZ of cement paste was investigated by comparing the DIC principal tensile strain maps of unreinforced and nanoreinforced specimens using the images acquired with the stereo-vision system

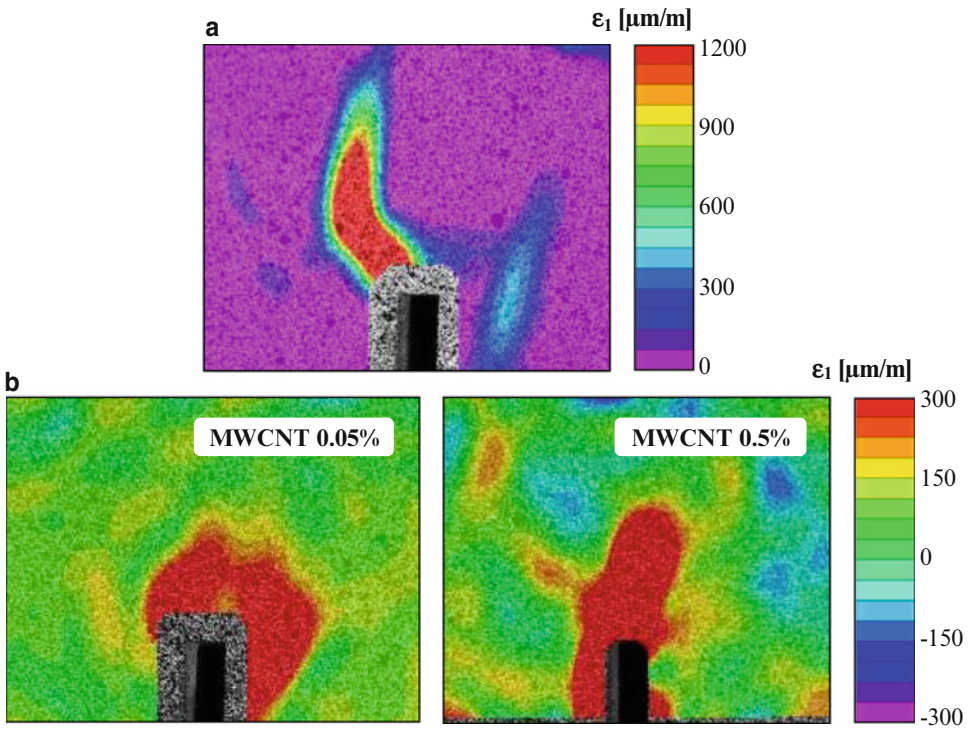

Fig. 10.5 Representative DIC principal tensile strain map in cement paste notched beam specimens in post-peak load stage: (**a**) unreinforced (control) beam; and (**b**) MWCNT-reinforced beams

in Fig. 10.1. Representative DIC principal tensile strain maps at the post-peak load stage (at the load-CMOD coordinates indicated by the circular markers in Fig. 10.3) are presented in Fig. 10.5.

The FPZ for unreinforced cement paste specimens is visualized as a relatively narrow and well-defined damage area at the crack tip. The FPZ for MWCNT-reinforced specimens is significantly larger and has a more progressive strain distribution in the vicinity of the notch, indicating a more damage tolerant zone where damage is more effectively distributed. This evidence is consistent with the load-CMOD curves presented in Fig. 10.3, the associated energy data summarized in Table 10.4, and the possible crack- and defect-bridging effect illustrated in Fig. 10.4.

10.4 Conclusions

Based on the experimental evidence presented in this paper, the following conclusions are drawn.

1) Acid-functionalization of MWCNTs resulted in well-dispersed nanoreinforcement in cement composite matrices for both a 0.05 and 0.5 % MWCNT concentration in weight of cement.
2) The incorporation of 0.05 % and 0.5 % of highly-dispersed acid-functionalized MWCNTs resulted in an average increase in compressive strength of cement mortar of 24 % and 41 %, respectively.
3) The fracture behavior of MWCNT-reinforced cement paste was assessed using three-point bending tests of notched beams. The incorporation of 0.05 % and 0.5 % of highly-dispersed acid-functionalized MWCNTs resulted in an average increase in peak flexural strength of 25 % and 22 %, respectively, and an average increase in flexural stiffness 93 % and 85 %, respectively. The load-CMOD curves show that the nanoreinforced specimens provide enhanced damage tolerance compared to the unreinforced counterparts, resulting in an increase in absorbed energy of 31 % and 28 % when using a 0.05 % and 0.5 % MWCNT concentration, respectively. Visual evidence from SEM analysis suggests the likelihood of a defect- and crack-bridging effect provided by the nanoreinforcement. There seem to be no additional benefit to damage tolerance in increasing the concentration of nanoreinforcement from 0.05 to 0.5 % in weight of cement.
4) The effect of MWCNTs on the FPZ of cement paste was evaluated based on DIC principal tensile strain maps around the beam notch. In the case of the unreinforced cement paste specimens, the FPZ is visualized as a narrow damage area, clearly reflecting a quasi-brittle behavior. In the case of the MWCNT-reinforced specimen, the FPZ is significantly larger and exhibits a more progressive strain distribution in the vicinity of the notch, providing promising experimental evidence of an enhanced damage tolerance as a result of incorporating well-dispersed and chemically compatible nanoreinforcement.

Acknowledgements The support of the University of South Carolina (USC) through a Promising Investigator Research Award (PIRA) to the third author, the State Center for Mechanics, Materials and Non-Destructive Evaluation, and the Magellan Program for undergraduate research is gratefully acknowledged. Special thanks are extended to: Ms. English Player (formerly undergraduate research assistant and USC Magellan mini-grantee), Prof. Navid Saleh and Mr. Nirupam Aich (formerly graduate student) for their assistance in processing of MWCNTs; and Prof. Michael Sutton, Prof. Anthony Reynolds, and Mr. Dan Wilhelm (USC Department of Mechanical Engineering) for their assistance in the use of the load test frame, CMOD sensor and DIC equipment. Correlated Solutions, Inc. (Columbia, SC) generously provided the Vic-3D v7 software used for the DIC analysis.

References

1. Yazdanbakhsh A, Grasley Z, Tyson B, Abu Al-Rub R (2012) Challenges and benefits of utilizing carbon nanofilaments in cementitious materials. J Nanomater 371927
2. Parveen S, Rana S, Fangueiro R (2013) A review on nanomaterial dispersion, microstructure and mechanical properties of carbon nanotube and nanofiber reinforced cementitious composites. J Nanomater 710175
3. Hilding J, Grulke EA, Zhang ZG, Lockwood F (2003) Dispersion of carbon nanotubes in liquids. J Disper Sci Technol 24(1):1–41
4. Vaisman L, Wagner HD, Marom G (2006) The role of surfactants in dispersion of carbon nanotubes. Adv Colloid Interfac 128:37–46
5. Makar JM, Beaudoin JJ (2004) Carbon nanotubes and their application in the construction industry. Sp Publ Roy Soc Chem 292:331–342
6. Musso S, Tulliani JM, Ferro G, Tagliaferro A (2009) Influence of carbon nanotubes structure on the mechanical behavior of cement composites. Compos Sci Technol 69(11):1985–1990
7. Cwirzen A, Habermehl-Cwirzen K, Nasibulin AG, Kaupinen EI, Mudimela PR, Penttala V (2009) SEM/AFM studies of cementitious binder modified by MWCNT and nano-sized Fe needles. Mater Charact 60(7):735–740
8. Metaxa ZS, Konsta-Gdoutos MS, Shah SP (2013) Carbon nanofiber cementitious composites: effect of debulking procedure on dispersion and reinforcing efficiency. Cement Concrete Comp 36:25–32
9. Nasibulina LI, Anoshkin IV, Nasibulin AG, Cwirzen A, Penttala V, Kauppinen EI (2012) Effect of carbon nanotube aqueous dispersion quality on mechanical properties of cement composite. J Nanomater 169262
10. Raki L, Beaudoin J, Alizadeh R, Makar J, Sato T (2010) Cement and concrete nanoscience and nanotechnology. Materials 3(2):918–942
11. Konsta-Gdoutos MS, Metaxa ZS, Shah SP (2010) Multi-scale mechanical and fracture characteristics and early-age strain capacity of high performance carbon nanotube/cement nanocomposites. J Cement Concrete Res 32:110–115
12. Wang B, Han Y, Liu S (2013) Effect of highly dispersed carbon nanotubes on the flexural toughness of cement-based composites. Constr Build Mater 42:8–12
13. Luo J, Duan Z, Li H (2009) The influence of surfactants on the processing of multi-walled carbon nanotubes in reinforced cement matrix composites. Phys Status Solidi A 206(12):2783–2790
14. Li GY, Wang PM, Zhao X (2005) Mechanical behavior and microstructure of cement composites incorporating surface-treated multi-walled carbon nanotubes. Carbon 43(6):1239–1245
15. Manzur T, Yazdani N (2010) Strength enhancement of cement mortar with carbon nanotubes. Transp Res Record 2142(1):102–108
16. Konsta-Gdoutos MS, Metaxa ZS, Shah SP (2010) Highly dispersed carbon nanotube reinforced cement based materials. Cement Concrete Res 40(7):1052–1059
17. Nochaiya T, Chaipanich A (2011) Behavior of multi-walled carbon nanotubes on the porosity and microstructure of cement-based materials. Appl Surf Sc 257(6):1941–1945
18. Orsuka K, Date H (2000) Fracture process zone in concrete tension specimen. Eng Fract Mech 65:111–131